

SINGLE STATION SIGMA FOR TURKISH STRONG MOTION STATIONS

Zehra Çağnan¹, and Sinan Akkar²

¹ Civil Engineering Department, TED University
Ziya Gökalp Caddesi, No:48, Kolej, 06420 Çankaya, Ankara, Turkey.
e-mail: zehra.cagnan@tedu.edu.tr

² Earthquake Engineering Department, Kandilli Observatory and Earthquake Research Institute,
Boğaziçi University
34684 Çengelköy, Istanbul, Turkey
sinan.akkar@boun.edu.tr

Keywords: Single station sigma, probabilistic seismic hazard assessment, ergodic assumption.

Abstract. *As ground motion observations over long enough time periods are unavailable for majority of sites, most of the ground motion prediction equations have been derived using observed data from multiple stations and seismic sources, and standard deviations (sigmas) of these equations are related to the statistics of the spatial variability of ground motion instead of temporal variability at a single site (ergodic assumption). This is one of the major shortcomings of carrying out site specific seismic hazard assessment with currently available ground motion prediction equations. In this study, we explore the variability at single sites within Turkey, decomposing sigma into different components so that the various contributions to the variability can be identified. The period and magnitude dependent standard deviation values obtained for Turkey using the ergodic assumption is changing between 0.56-0.82 ln units [1]. When single stations are considered instead, standard deviation estimates are reduced by 20%. Through the restriction of the analysis to a particular seismic source (i.e. North Anatolian Fault zone), the standard deviation values obtained for Turkey by [1] are further shown to reduce by about 10-20% depending on the spectral period under consideration. Implications of these findings for the seismic hazard of Istanbul district are further discussed within the scope of this study.*

1 INTRODUCTION

Ground motion prediction equations (GMPE) are based on datasets of ground motion parameters recorded at multiple stations, the source of which are different earthquakes generated by various tectonic sources. These equations that are utilized to predict ground motion at a specific site, describe its distribution (log-normal distribution) in terms of a median and a logarithmic standard deviation. [2] explained aleatory variability as that “inherent to the unpredictable nature of future events and cannot be reduced by collection of additional information”. Whereas they described epistemic variability as that “is due to incomplete knowledge and data about the physics of the earthquake process and can be reduced to zero with sufficient knowledge (at least theoretically)”. Although it is usually envisioned that through standard deviation of ground motion prediction equations, only aleatory variability of ground motion is represented that is not the case in reality.

When ground motion prediction equations are utilized as part of seismic hazard assessment studies, an inherent assumption is made: the ground motion variability obtained based on a global (or regional) dataset is the same as the variability of ground motion caused by a single source at a single site. This assumption has been referred to as the ergodic assumption (i.e. [3-5]). Over the last decade, the availability of recorded ground motions at single sites caused by multiple earthquakes originating from the same tectonic sources has allowed researchers to estimate what is referred to as nonergodic standard deviation (also referred to as single station standard deviation or single station sigma) of ground motion [6-13]. These studies illustrated in general that average nonergodic standard deviations are lower than their ergodic equivalents. Quantification of nonergodic standard deviation enables elimination of epistemic site to site, path to path and source to source variability from the ground motion prediction equation standard deviation hence is a step forward towards quantification of true aleatory variability of ground motion at a specific site. For an ideal probabilistic seismic hazard assessment study, standard deviation of ground motion prediction equation should only represent aleatory variability of ground motion and epistemic uncertainty should be captured through following the logic tree approach.

Ground motion standard deviation exerts a strong influence on the results of the probabilistic seismic hazard analysis, even small variations causing considerable differences on hazard results particularly at long return periods [14]. Hence computing nonergodic standard deviation, that offers more realistic quantification of ground motion variability at a specific site has become particularly important in the evaluation of ground motions utilized for the design of critical facilities especially such as nuclear power plants [11, 15-16]. The focus of this study is to compute nonergodic standard deviation based on the Turkish strong motion database and determine the effect of using it instead of ergodic standard deviation on seismic hazard estimates for the Fatih-Kadikoy districts of Istanbul.

2 THEORETICAL BACKGROUND

Following the notation of [17] in this study, total residuals (Δ_{es}) are defined as the difference between recorded ground motions and the values predicted by a ground motion prediction equation in log units. Two main terms: between-event (δB_e) and within-event (δW_{es}) terms can be thought of contributing to these total residuals:

$$\Delta_{es} = \delta B_e + \delta W_{es} \quad (1)$$

in which the subscripts denote an observed ground motion parameter corresponding to an event e at station s . Between-event term represents the average shift, corresponding to an in-

dividual earthquake - e , of the observed ground motions from corresponding median estimates of ground motion prediction equation. Within-event term on the other hand represents the difference between an individual observation at station s from the earthquake-specific median prediction. The between-event and within-event residuals are independent normally distributed random variables with zero means and standard deviations τ and ϕ , respectively. The between-event standard deviation, τ , represents the earthquake to earthquake variability reflecting influence of factors such as stress drop and variation of slip in space and time that are not captured by ground motion prediction equations through inclusion of parameters such as magnitude, style of faulting and source depth. The within-event standard deviation, ϕ , represents the record to record variability reflecting influence of factors such as crustal heterogeneities, deeper geological structures, near-surface layering that are not captured by ground motion prediction equations through inclusion of parameters such as distance, site classification.

The within-event residuals can be further divided into two terms:

$$\delta W_{es} = \delta S2S_s + \delta WS_{es} \quad (2)$$

$\delta S2S_s$, site term, represents the average within-event residual at each station, and δWS_{es} is the site- and event-corrected residual. $\delta S2S_s$ and δWS_{es} are zero mean normally distributed random variables as well with standard deviations ϕ_{S2S} and ϕ_{SS} , respectively. The uncertainty in the site term can be reduced with additional information (i.e. ground motion observations, analytical site specific response models). The site term represents the systematic deviation of the observed amplification at a station site from the median amplification predicted by the site amplification model of the ground motion prediction equation. The site- and event-corrected residual on the other hand represents unexplained path and radiation pattern effects. The site term can be computed as:

$$\delta S2S_s = \frac{1}{NE_s} \sum_{e=1}^{NE_s} \delta W_{es} \quad (3)$$

where NE_s stands for the number of earthquakes, e , recorded by station s and the event-corrected single station standard deviation can be computed as:

$$\phi_{ss} = \sqrt{\frac{\sum_{s=1}^{NS} \sum_{e=1}^{NE_s} (\delta W_{es} - \delta S2S_s)^2}{(\sum_{s=1}^{NS} NE_s - 1)}} \quad (4)$$

where NS represents the total number of stations or sites considered in the computation of event corrected single station standard deviation. As the site term is unique for a specific site, the event corrected single station standard deviation is unique as well. For a specific site, it is possible to compute an estimate of event corrected single station ($\phi_{ss,s}$) by letting NS of equation 4 above to be equal to 1. Average of $\phi_{ss,s}$ estimates for a number of stations approximately equals to ϕ_{ss} for a region containing these stations.

The between-event residuals can also be divided into two terms:

$$\delta B_e = \delta L2L_l + \delta B_{el} \quad (5)$$

$\delta L2L_l$, source term, represents the average between-event residual for each source region, l , and δB_{el} is the source-corrected between-event residual. $\delta L2L_l$ and δB_{el} are zero mean normally distributed random variables as well with standard deviations τ_{L2L} and τ_{SS} , respectively. The source term represents the systematic deviation of the ground motion for an earthquake in a single region from the median predicted by the ground motion prediction equation. The source-corrected between-event residual on the other hand represents unexplained source and slip pattern effects. The source term can be determined as:

$$\delta L2L_l = \frac{1}{NE_l} \sum_{e=1}^{NE_l} \delta B_e \quad (6)$$

where NE_l stands for the number of earthquakes, e , associated with the source region l and the source-corrected between-event standard deviation can be computed as:

$$\tau_{ss} = \sqrt{\frac{\sum_{e=1}^{NE_l} (\delta B_e - \delta L2L_l)^2}{(NE_l - 1)}} \quad (7)$$

Finally, the single source single station standard deviation can be computed by combining event corrected single station standard deviations with source corrected between-event standard deviations through:

$$\sigma_{ss} = \sqrt{\varphi_{ss}^2 + \tau_{ss}^2} \quad (8)$$

In the process of computation of single source single station standard deviation only two components (i.e. source and site effects) of the total ground motion variability that are not representative of the variability of future ground motion observations at a specific site are removed from the ground motion prediction equation standard deviation (total standard deviation). Hence it can be said that single source single station standard deviation is only partially nonergodic. To get a fully nonergodic standard deviation, all of the components (i.e. path effects in addition to site and source effects) of the total ground motion variability that are not representative of the variability of future observations of ground motion at a single site must be removed. Within the scope of this study, we did not make an effort towards removing the path effects from site- and event-corrected residuals, δWS_{es} , as currently the stations of the Turkish strong motion network do not possess the necessary level of density that would enable such an analysis.

Components of Variability	Definition
Total standard deviation	$\sigma = \text{std}(\Delta_{es}) = \sqrt{\tau^2 + \varphi^2}$
Single source single station standard deviation	$\sigma_{ss} = \sqrt{\tau_{ss}^2 + \varphi_{ss}^2}$
Between-event standard deviation	$\tau = \text{std}(\delta B_e)$
Within-event standard deviation	$\varphi = \text{std}(\delta W_{es})$
Site to site variability	$\varphi_{S2S} = \text{std}(\delta S2S_s)$
Event corrected single station standard deviation	$\varphi_{SS} = \text{std}(\delta WS_{es})$

Source to source variability	$\tau_{L2L}=\text{std}(\delta L2L_i)$
Source corrected between-event standard deviation	$\tau_{SS}=\text{std}(\delta B_{el})$

Table 1: Components of the Variability of Ground Motion Prediction Equations (std below stands for the standard deviation operator)

3 DATABASE

In order to constrain event corrected single station standard deviation and source corrected between-event standard deviation values for Turkey, the Turkish strong motion database developed within the scope of the EMME project was utilized [18]. This database includes 1190 strong motion records from 203 earthquakes. The accelerograms are recorded at 304 strong-motion stations.

All accelerograms belonging to this database are uniformly processed following the procedure outlined in [19]. The maximum spectral period values below which each accelerogram can be utilized were also determined from the empirical formulations given in [19]. However, after carrying out a preliminary study in order to obtain more stable results towards the higher end of the considered period range it was decided to increase these maximum spectral period values by 25% and to utilize the following empirical relations instead: $1.0T_c$ for rock, $1.125T_c$ for stiff soil and $1.213T_c$ for soft soil sites in the case of digital records; $0.813T_c$ for rock, $0.813T_c$ for stiff soil and $0.875T_c$ for soft soil sites in the case of analogue records where T_c represents long period cut off filter periods used when processing the records. The moment magnitude (M_w) information available in the database was obtained from double couple fault plane solutions for some events and from magnitude conversion equations for others. The ruptured fault geometry information from the literature or its estimates from empirical relationships of [20] were utilized to compute the Joyner and Boore distances (R_{JB}) included in the database. All the record entries of this database have corresponding measured average shear wave velocity for the upper 30m of soil profile, V_{s30} , values [21]. An upper limit for depth in accordance with the study of [22] was selected for this database so that it only includes shallow event data. The magnitude, distance, site class and style of faulting based distributions of the strong motion data used in this study are given in the figures below.

In order to obtain stable event corrected single station sigma values, initially only data recorded by stations with at least 5 records were utilized. This is referred to as the main database and consists of 736 records from 174 earthquakes that are recorded by 84 different stations. The choice of employing this minimum number of records per station limitation depends on a detailed parametric study. In this parametric study, various least number of records per station limitations (i.e. none, 5, 10, 15, 20 records) were adopted and effects of this parameter on ϕ (or ϕ_{ss}) vs. spectral period relationships, distributions of $\phi_{ss,s}$ values at various spectral periods, variability of $\phi_{ss}/\phi_{ss,s}$ ratios were studied. Details of this parametric study will not be shared as part of this manuscript due to space limitations; however we will utilize its aforementioned conclusion in the rest of this work. Further to be able to compute a stable single source between-event standard deviation value for the North Anatolian Fault (NAF), records of events that are associated with NAF were selected from the main database. This new database will be referred to as the NAF database in the rest of this manuscript. It consists of 370 records from 26 earthquakes that are recorded by 68 unique stations.

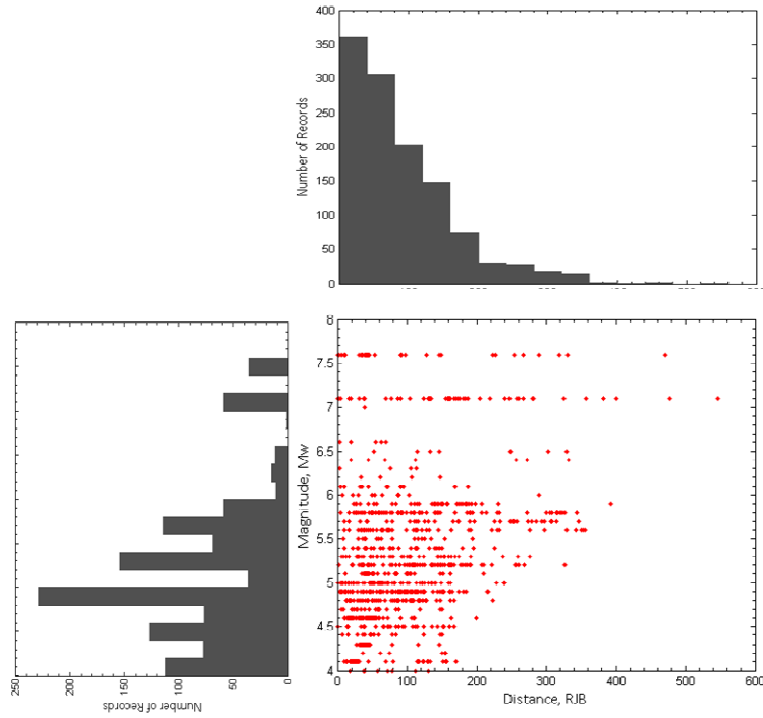


Figure 1: Distribution of records in the Turkish strong motion database with respect to the moment magnitude, M_w and Joyner and Boore distance, R_{JB} parameters. Majority of records in the database have corresponding moment magnitude, M_w values in the range 4.0-6.0 with a median value of 5.0 and corresponding Joyner and Boore distance, R_{JB} values in the range 0-100 km with a median value of 65 km. Distributions of records in the database with respect to site class and style of faulting parameters are not uniform either. Majority of records having corresponding NEHRP C or D site classes and strike-slip or normal styles of faulting.

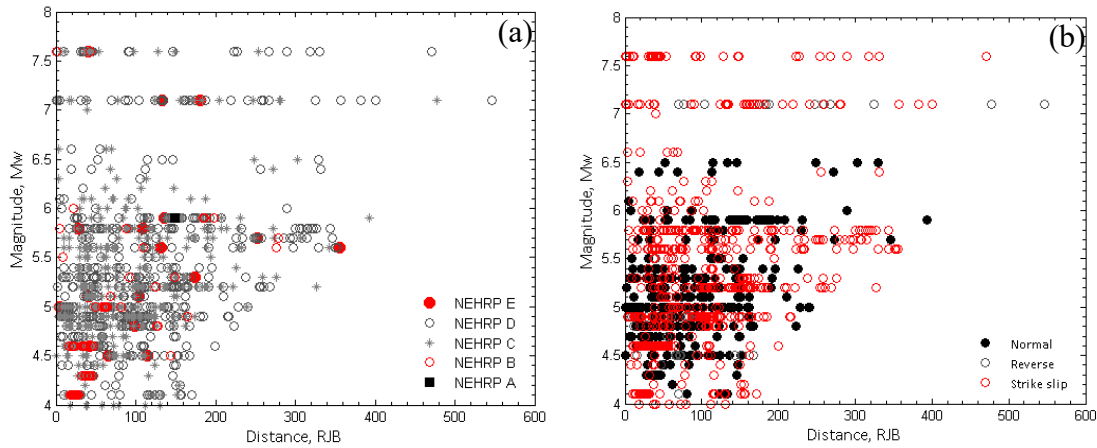


Figure 2: Distribution of records in the Turkish strong motion database with respect to (a) site class and (b) style of faulting parameters. National Earthquake Hazards Reduction Program site classification scheme is adopted in this study [23]: NEHRP Class E – $V_{s30} < 180$ m/s, NEHRP Class D – $180 \text{ m/s} < V_{s30} < 360$ m/s, NEHRP Class C – $360 \text{ m/s} < V_{s30} < 760$ m/s, NEHRP Class B – $760 \text{ m/s} < V_{s30} < 1500$ m/s, NEHRP Class A – $1500 \text{ m/s} < V_{s30}$.

4 EVENT CORRECTED SINGLE STATION STANDARD DEVIATION (ϕ_{ss})

Towards computation of ϕ_{ss} values, firstly horizontal ground-motion estimates of [1] GMPE corresponding to each entry of the Turkish strong motion database was obtained. By subtracting these median estimates from the ground motion observations of the Turkish strong motion database, total residuals were computed. Total residuals were then separated into between-event and within-event residuals through following [24]. And as the final step, by following the definitions of within-event standard deviation (ϕ), event corrected single station standard deviation (ϕ_{ss}), event corrected single station standard deviation for a specific station/site ($\phi_{ss,s}$) as given in the theoretical background part of this manuscript, these standard deviation values were computed. Distributions of within-event residuals computed based on the main strong motion database with R_{JB} and V_{S30} are shown in figures 3 and 4 respectively for peak ground acceleration (PGA), peak ground velocity (PGV) and pseudo spectral acceleration (PSA) at spectral periods of 0.1 and 2s. Expectedly no trends are observable with the parameters R_{JB} and V_{S30} .

[1] suggests M_w dependent equations for the estimation of within-event standard deviation. However within the scope of our study, a weak magnitude dependency was observed for event corrected single station standard deviations corresponding to spectral period values not exceeding 0.75s and for source corrected between-event standard deviations corresponding to all spectral periods. As a result magnitude independent event corrected single station standard deviations and source corrected between-event standard deviations are suggested (table 2). In order to preserve the [1] suggested within-event standard deviation-spectral period model for the event corrected single station standard deviations, the maximum likelihood approach was adopted. In figure 5, variation of within-event standard deviation and event corrected single station standard deviation values with spectral period is given for $M_w < 6.0$ and $M_w > 6.5$ events. Figure 5 suggests at least 50% reduction in within-event standard deviation values as a result of excluding the site to site variability.

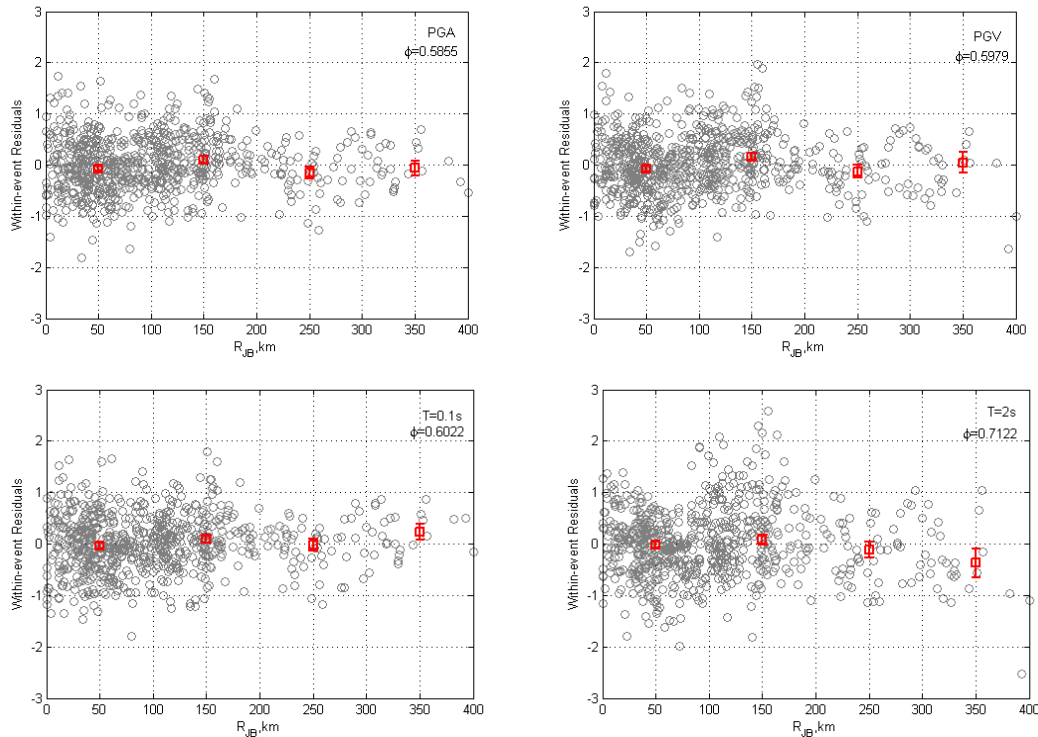


Figure 3: Distribution of within-event residuals with Joyner and Boore distance for PGA, PGV and PSA at spectral periods of 0.1 and 2s. Error bars represent the mean and 95th-percentile confidence limits of the mean binned residuals.

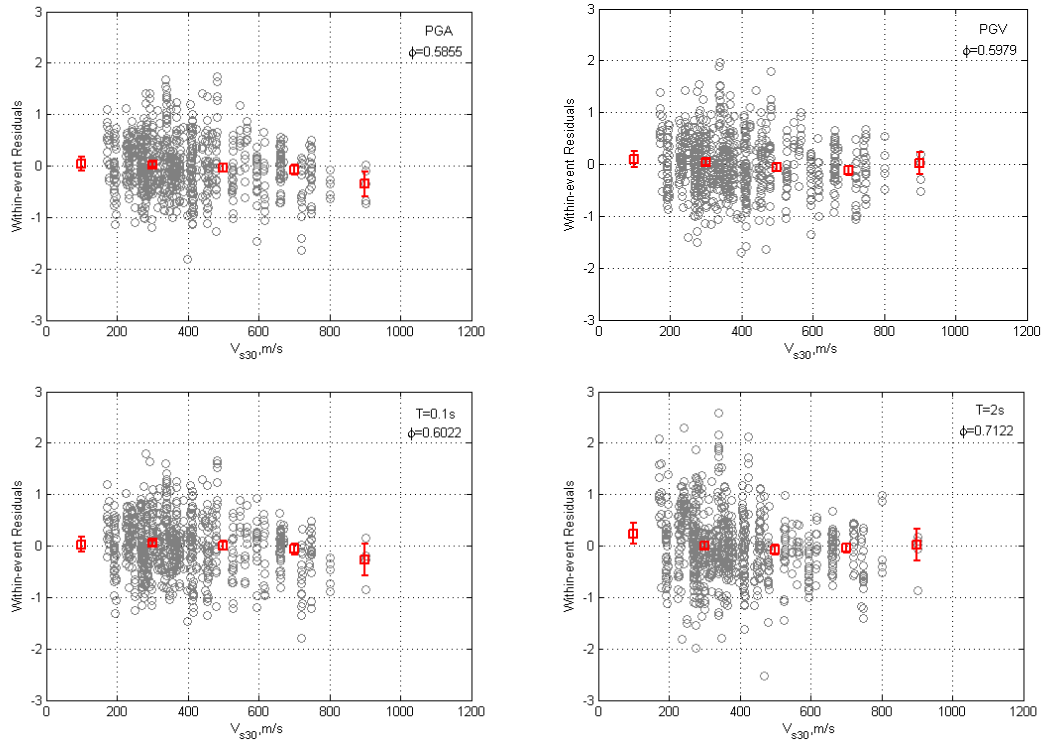


Figure 4: Distribution of within-event residuals with V_{s30} for PGA, PGV and PSA at spectral periods of 0.1 and 2s. Error bars represent the mean and 95th-percentile confidence limits of the mean binned residuals.

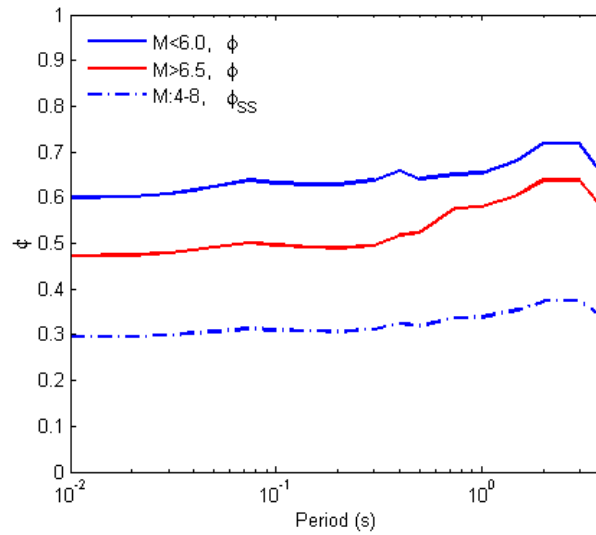


Figure 5: Variation of within-event standard deviation (ϕ) and event corrected single station standard deviation (ϕ_{ss}) with spectral period for $M_w < 6.0$ and $M_w > 6.5$ events.

Finally, the epistemic uncertainty estimate of this study associated with ϕ_{ss} values is 0.10 that is in close agreement with those suggested by [6-9, 11 and 13]. The same epistemic uncertainty value was adopted for τ_{ss} in this study.

Period	b_1	ϕ_{ss}	τ_{ss}
PGA	2.02431	0.295	0.191
0.01	2.03625	0.295	0.191
0.02	2.06791	0.296	0.192
0.03	2.16509	0.299	0.192
0.04	2.31478	0.303	0.194
0.05	2.4642	0.307	0.196
0.075	2.98459	0.313	0.213
0.1	3.09176	0.31	0.217
0.15	3.26922	0.308	0.215
0.2	3.19846	0.307	0.214
0.3	2.62229	0.311	0.205
0.4	2.11359	0.324	0.208
0.5	1.60036	0.32	0.207
0.75	0.76360	0.337	0.200
1	0.39277	0.339	0.193
1.5	-0.01037	0.354	0.188
2	0.00454	0.373	0.174
3	-0.07912	0.373	0.190
4	0.03525	0.334	0.165
PGV	5.72860	0.293	0.171

Table 2: Period dependent coefficients for event corrected single station standard deviation, source (NAF) corrected between-event standard deviation and b_1 values for the [1] GMPE in the case of $M_w < 6.5$ events.

5 SOURCE CORRECTED BETWEEN-EVENT STANDARD DEVIATION (τ_{ss})

By utilizing the NAF database together with equations 6 and 7, the source term corresponding to the North Anatolian Fault and the source corrected between-event standard deviation (τ_{ss}) are estimated in this part of the study. Distributions of between-event residuals with magnitude obtained by utilizing the main database are given for PGA, PGV and PSA at spectral periods of 0.1 and 0.2s in figure 6. Expectedly, no trend is observable in these distributions when positions of the error bars with respect to the zero residual line are considered. In figure 7, distributions of between-event residuals with magnitude obtained by utilizing the NAF database only are given instead for the same spectral periods of above. The shift of mean between-event residuals for $M_w < 6.5$ events towards positive values is apparent in the case of PGA, PGV and 0.1s PSA plots. This is an indication that when NAF originated events considered only, there is a non zero source term. The mean between-event residuals for the two $M_w > 6.5$ events of the database on the other hand have negative values for all spectral periods considered. These two correspond to the 1999 Kocaeli and Duzce earthquakes that are characterized with lower than expected peak acceleration values as thoroughly discussed in the literature until now. We are therefore suggesting application of the estimated source term only to $M_w < 6.5$ events until magnitude saturation effects are better understood for the NAF source by capturing more records of large magnitude events in the future. In order to obtain source corrected between-event residuals, the estimated source term for NAF is subtracted from the between-event residuals of $M_w < 6.5$ events as suggested by equation 5. The source corrected between-event residuals and their distribution with magnitude for PGA, PGV and PSA at spectral periods of 0.1 and 0.2s are given in figure 8. By subtracting the source term, error bars approached to the zero residual line once again. It is further possible to reflect the esti-

mated source term to the [1] suggested GMPE and by doing so it would be possible to convert it from a regional GMPE to a local GMPE specifically suitable for the Marmara region. This modification can be achieved by suggesting updated b_1 coefficients for the [1] GMPE (listed in table 2); only to be used in the case of $M_w < 6.5$ events. For $M_w > 6.5$ events, use of original b_1 coefficients as proposed by [1] is recommended.

With source corrected between-event residuals, τ_{SS} values were further computed corresponding to different spectral periods. As magnitude dependency for τ_{SS} values was not observed in this study, they are suggested in table 2 as constants although between-event standard deviations, τ , of [1] have magnitude dependency. In figure 9, variation of between-event standard deviation and source corrected between-event standard deviation values with spectral period is given for $M_w < 6.0$ and $M_w > 6.5$ events. In order to preserve the [1] suggested between-event standard deviation-spectral period model for the source corrected between-event standard deviation; the maximum likelihood approach was adopted once again. Figure 9 suggests 10-55% reduction in between-event standard deviation values resulting from excluding the source effect.

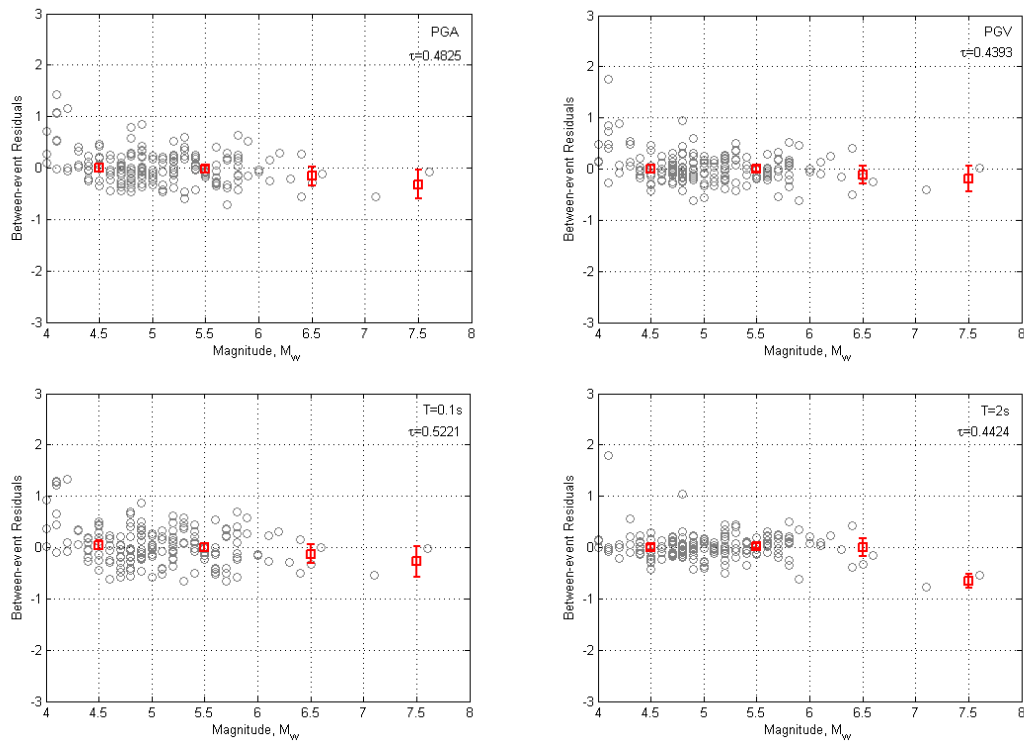


Figure 6: Distribution of between-event residuals obtained based on the main database with moment magnitude, M_w for PGA, PGV and PSA at spectral periods of 0.1 and 2s. Error bars represent the mean and 95th-percentile confidence limits of the mean binned residuals.

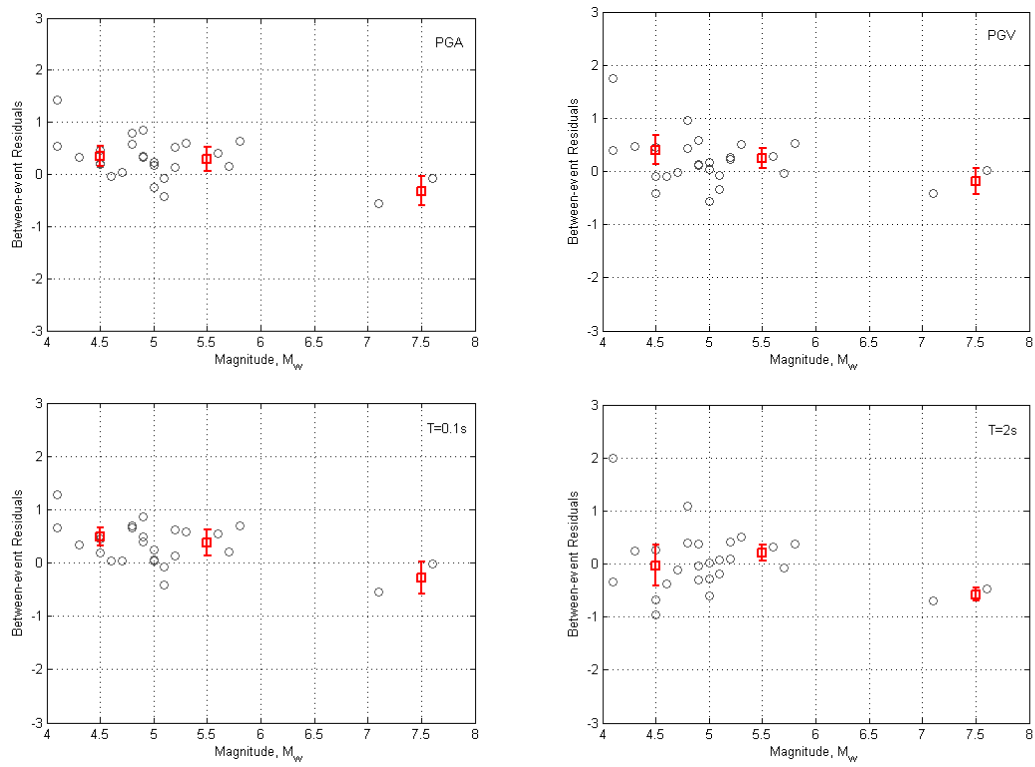


Figure 7: Distribution of between-event residuals obtained based on the NAF database with moment magnitude, M_w for PGA, PGV and PSA at spectral periods of 0.1 and 2s. Error bars represent the mean and 95th-percentile confidence limits of the mean binned residuals.

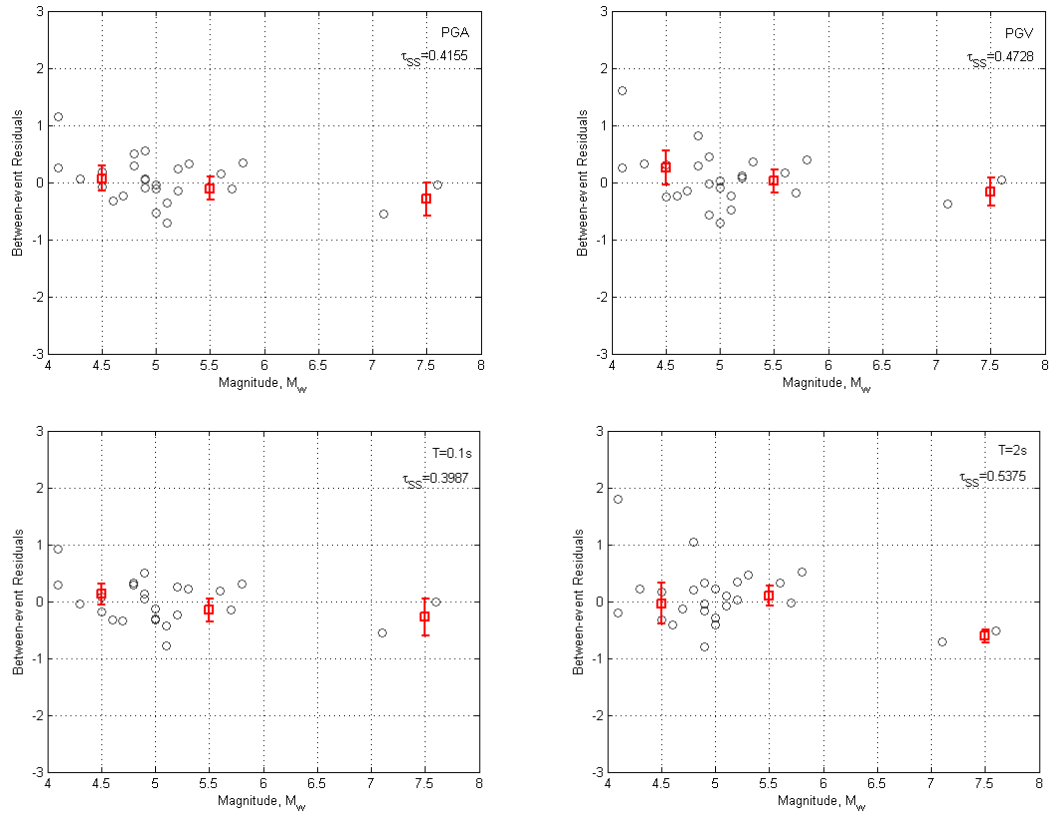


Figure 8: Distribution of source corrected between-event residuals obtained based on the NAF database with moment magnitude, M_w for PGA, PGV and PSA at spectral periods of 0.1 and 2s. Error bars represent the mean and 95th-percentile confidence limits of the mean binned residuals.

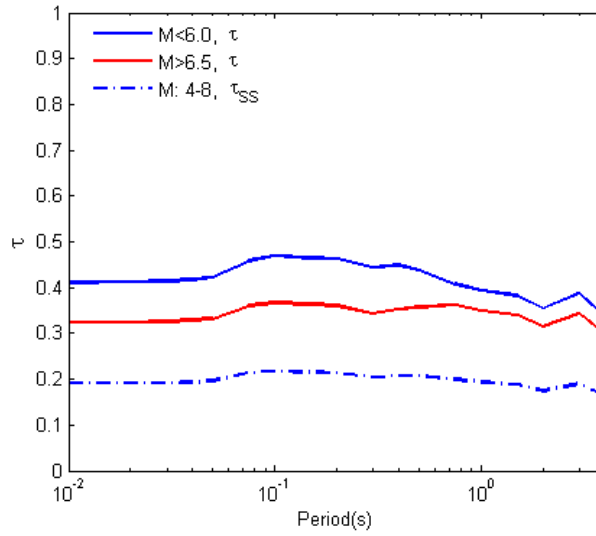


Figure 9. Variation of between-event standard deviation (τ) and source corrected between-event standard deviation (τ_{ss}) with period for $M_w < 6.0$ and $M_w > 6.5$ events.

6 EFFECT OF SINGLE SOURCE SINGLE STATION STANDARD DEVIATION (σ_{ss}) ON SEISMIC HAZARD CURVE

In order to observe the effect on seismic hazard estimates of utilizing σ_{ss} rather than σ , the probabilistic seismic hazard assessment software developed by [25] that is based on the Monte Carlo simulation approach was used. Following the suggestions of [26], the Princes Islands and Marmara segments of the North Anatolian Fault beneath the Marmara Sea were considered as the major source of seismicity for Istanbul (figure 10). Within the scope of this study, seismic hazard for the Fatih and Kadikoy districts of Istanbul was assessed (figure 10). A slip rate of 20mm/yr producing characteristic earthquakes of M_w 6.9-7.3 was assumed for both segments. The probability density function on event magnitude was assumed to follow the maximum magnitude model and the rate of event occurrence was modeled with Poisson process [27]. Within the scope of this study, we used a 100 year catalogue period and ran 10,000 simulations that resulted in a total catalogue interval of 1 million years. [25]'s probabilistic seismic hazard assessment software is capable of taking into account the effects of spatial correlation as well as near fault directivity for ground motion simulations however spatial correlation and near fault directivity were not incorporated into the current study. A cell size of $0.005^\circ \times 0.005^\circ$ was used (figures 11 and 15). In the first part of the study, a fixed soil condition with a V_{s30} value of 760m/s (corresponding to NEHRP B-C boundary) for the whole region of interest was used. In the second part, however, actual soil conditions deducted from the previously completed microzonation studies were used: a unique V_{s30} value was assigned for each cell [28].

The seismic hazard curves developed by utilizing total standard deviation, σ , as well as single source single station standard deviation, σ_{SS} , for 4 separate sites are given in figure 13. These sites were selected such that they represent high, moderate and low seismic hazard levels for the region of interest (figure 11 and figure 14a). At an annual exceedance rate level of 10^{-4} , up to 20% overestimations in seismic hazard estimates by utilizing total standard deviation, σ , instead of single source single station standard deviation, σ_{SS} , were detected when PGA is the intensity measure utilized.

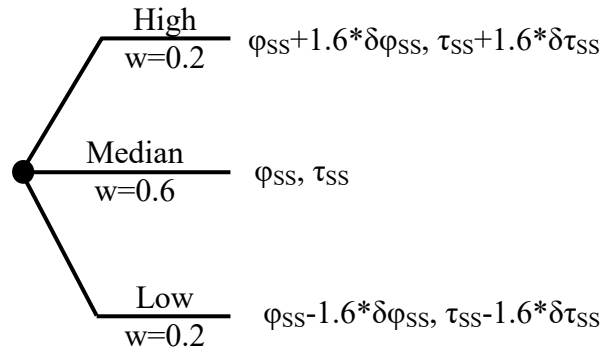


Figure 12: Schematic representation of the sigma model of this study.

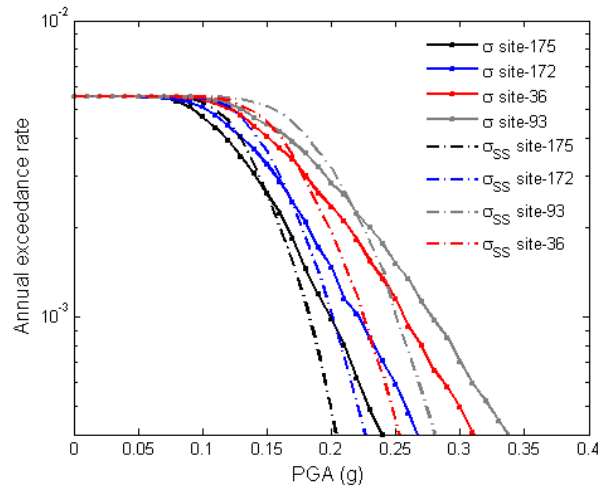


Figure 13: Effect of using σ vs σ_{SS} on seismic hazard curves for grids 36, 93, 172 and 175 (exact locations indicated in figure 11).

In the second part of the study in order to reflect the effect of site term on the results as well, site of a strong motion station was selected and seismic hazard estimates corresponding to actual site conditions were obtained. The selected strong motion station site is shown in figure 15. Data recorded (10 records) by this station is part of the main and NAF strong motion databases of this study. According to these databases, the measured V_{S30} value corresponding to this station site is 338.6 m/s, which corresponds to NEHRP D type soil condition. Based on these 10 records belonging to the station site, corresponding site term, δS_{2S} , was estimated to be 0.5094 and epistemic uncertainty associated with the site term, $\delta\phi_{S2S}$, to be 0.12 when PGA is used as the intensity measure.

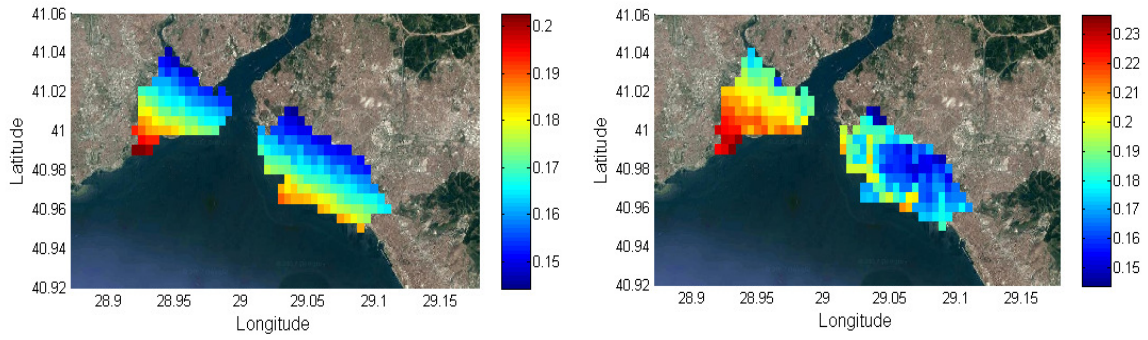


Figure 14. Median PGA (g) distributions for the Fatih-Kadikoy districts of Istanbul when (a) $V_{s30}:760\text{m/s}$ site condition for all grids, (b) actual site condition for all grids and total standard deviation, σ , parameters were utilized in seismic hazard computations.

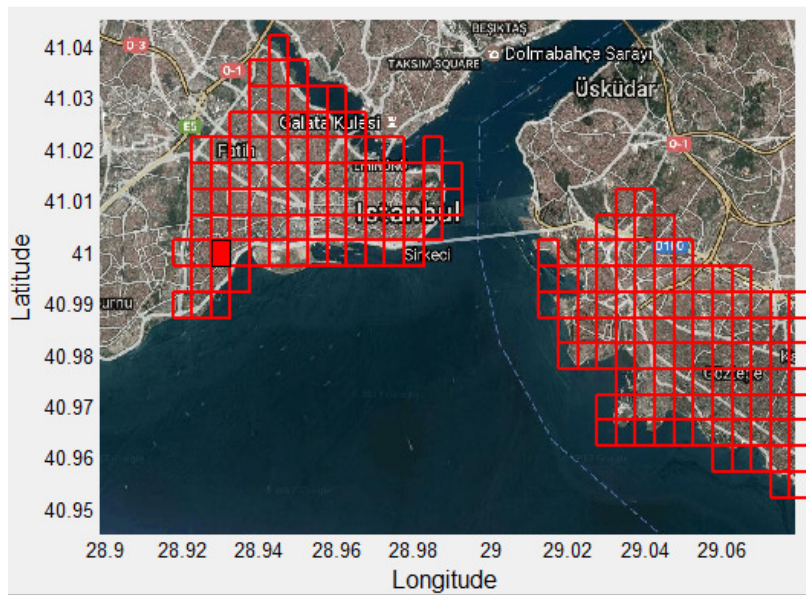


Figure 15: 0.005° by 0.005° grid covering Fatih-Kadikoy districts of Istanbul. Seismic hazard curve with site effect reflected fully was developed specifically for the 126 numbered grid which corresponds to a strong motion site (red shaded grids).

In figure 17, the seismic hazard curve obtained for the station site by utilizing the total standard deviation, σ , as well as the site amplification model of [1] is given. Figure 17 also includes the seismic hazard curve obtained for the station site when single source single station standard deviation, σ_{ss} , (figure 12) was utilized together with the site amplification model of [1] and estimated site term, $\delta S2S$, as given above. The epistemic uncertainties associated with the site and source terms were taken into account through the median logic tree model (figure 16). Figure 17 indicates that for the specific site considered, at an annual exceedance rate of 10^{-4} up to 20% underestimation in seismic hazard estimates can be obtained by utilizing total standard deviation, σ , instead of single source single station standard deviation, σ_{ss} , when PGA is the intensity measure used.

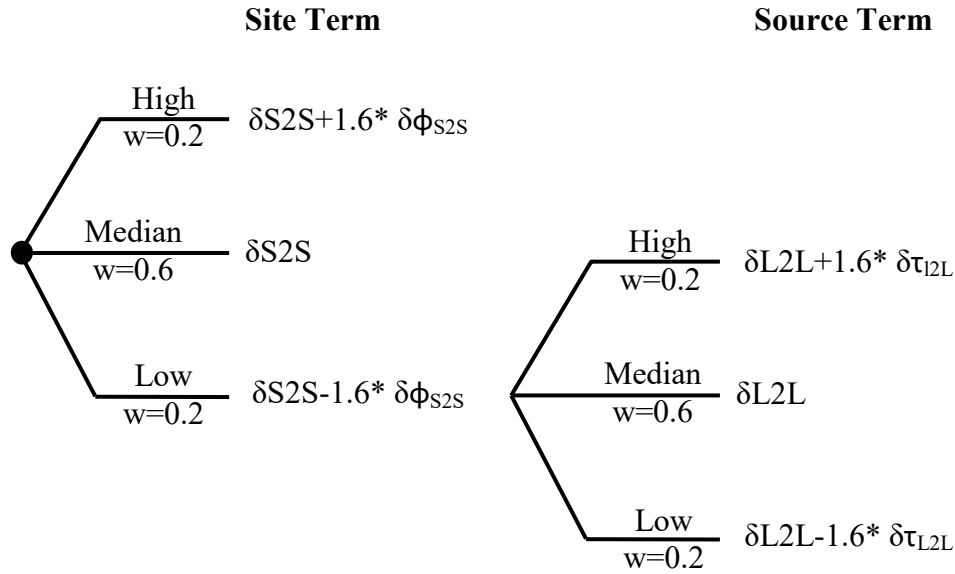


Figure 16: Schematic representation of the median logic tree model of this study.

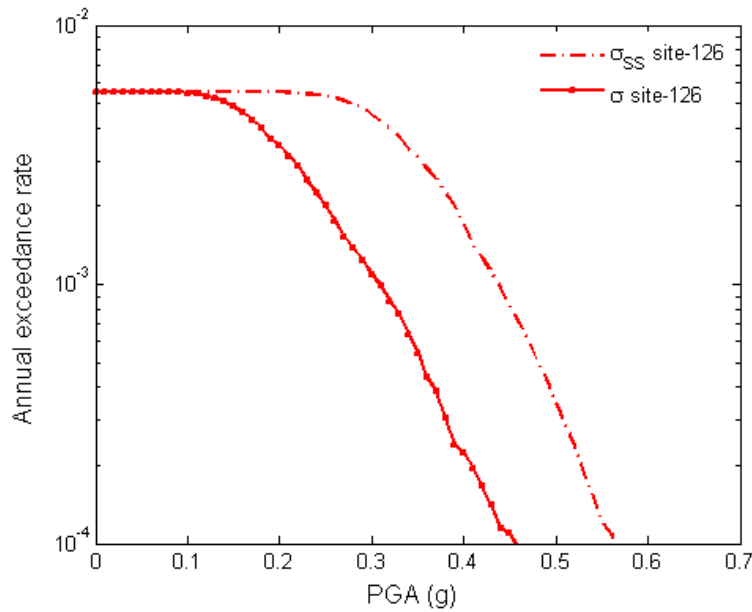


Figure 17: Effect of using σ vs σ_{SS} on the seismic hazard curve of investigated strong motion site (exact location indicated in figure 15).

7 CONCLUSIONS

Main conclusions of this study are the following:

- The spectral period and magnitude dependent standard deviation obtained for Turkey using the ergodic assumption is changing between 0.56-0.82 ln units [1]. This range reduces to about 0.42-0.56 ln units when single station standard deviation is considered (minimum of 20% reduction).
- When results of this study are compared with results of other single station sigma studies (i.e. [6, 8 and 9]), we observe that standard deviation values with and without

the ergodic assumption computed based on the Turkish strong motion database are larger than the corresponding standard deviation values computed based on other databases. This suggests that by improving event and station metadata of the Turkish strong motion database as well as the number of records per station parameter, standard deviation values can further be reduced in the future.

- Restricting the analysis to the North Anatolian Fault seismic source only, enabled reducing (single source) single station standard deviation values to a range of 0.34-0.42 ln units. This result is significant as it suggests that standard deviation values at a particular site due to a specific source may be reduced by about 40-50% depending on the spectral period under consideration in comparison to the total standard deviation values of 0.56-0.82 ln units for Turkey.
- As utilizing single source single station standard deviation values instead of total standard deviation values as part of the seismic hazard assessment exercises carried out also lead to encouraging results, new efforts in strong motion data collection are strongly suggested for Turkey in addition to revision of currently available event and station metadata.

REFERENCES

- [1] Kale Ö, Akkar S, Ansari A, Hamzehloo H. A ground-motion predictive model for Iran and Turkey for horizontal PGA, PGV and 5%-damped response spectrum: Investigation of possible regional effects. *Bull. Seismol. Soc. Am.* 103, no. 2A, 963-980, 2015.
- [2] Toro G, Abrahamson N, Schneider J. Letter to the editor, *Seismological Research Letters* 68, 3, 481-482, 1997.
- [3] Anderson J G and Brune J N. Probabilistic seismic hazard assessment without the ergodic assumption, *Seismological Research Letters* 70, 19-28, 1999.
- [4] Douglas J. Earthquake ground motion estimation using strong motion records: A review of equations for the estimation of peak ground acceleration and response spectral ordinates. *Earth Sci. Rev.* 61, 43-104, 2003.
- [5] Strasser F O, Abrahamson N A and Bommer J J. Sigma: Issues, insights and challenges. *Seismological Research Letters* 80, 40-54, 2009.
- [6] Atkinson G M. Single-station sigma. *Bulletin of Seismological Society of America* 96, 446-455, 2006.
- [7] Morikawa N, T Kanno, A Narita, H Fujiwara, T Okumura, Y Fukushima and A Gurpinar. Strong motion uncertainty determined from observed records by dense network in Japan. *Journal of Seismology* 12, 529-546, 2008.
- [8] Lin P, N Abrahamson, M Walling, C-T Lee, B Chiou and C Cheng. Repeatable path effects on the standard deviation for empirical ground-motion models. *Bulletin of Seismological Society of America* 101, 2281-2295, 2011.
- [9] Rodriguez-Marek A, G A Montalva, F Cotton and F Bonilla. Analysis of single-station standard deviation using the KiK-net data. *Bulletin of Seismological Society of America* 101, 1242-1258, 2011.

- [10] Rodriguez-Marek A, F Cotton, NA Abrahamson, S Akkar, L Al Atik, B Edwards, G A Montalva and H M Dawood. A model for single station standard deviation using data from various tectonic regions. *Bulletin of Seismological Society of America* 103, 6, 3149–3163, 2013.
- [11] Rodriguez-Marek A, E M Rathje, J J Bommer, F Scherbaum and P J Stafford. Application of single station sigma and site response characterization in a probabilistic seismic hazard analysis for a new nuclear site. *Bulletin of Seismological Society of America* 104, 4, 1601–1619, 2014.
- [12] Edwards B and D Fäh. A stochastic ground-motion model for Switzerland. *Bulletin of Seismological Society of America*, 103, 1, 2013.
- [13] Luzi L, D Bindi, R Puglia, F Pacor and A Oth. Single station sigma for Italian strong motion stations. *Bulletin of Seismological Society of America* 104, 1, 467-483, 2014.
- [14] Bommer J J and N A Abrahamson. Why do modern probabilistic seismic-hazard analyses often lead to increased hazard estimates? *Bulletin of Seismological Society of America* 96, 1967–1977, 2006.
- [15] Abrahamson N A and Hollenback J C. Application of single station sigma ground motion prediction equations in practice. Proceedings of the 15th world Conference on Earthquake Engineering, Lisboa, Portugal, 2012.
- [16] Bommer J, Coppersmith JK, Coppersmith RT, Hanson KL, Mangongolo A, Neveling J, Rathje EM, Rodriguez-Marek A, Scherbaum F, Shelembe R, Stafford P, Strasser FO. A SSHAC Level 3 probabilistic seismic hazard analysis for a new building nuclear site in South Africa. *Earthquake Spectra* 31, no. 2, 661-698, 2015.
- [17] Al Atik L, N Abrahamson, F Cotton, F Scherbaum J Bommer and N Kuehn. The variability of ground-motion prediction models and its components, *Seismological Research Letters* 81, 794–801, 2010.
- [18] Akkar S, Kale Ö, Ansari A, Durgaryan R, Askan Gündoğan A, Hamzehloo H, Harmandar E, Tsereteli N, Waseem M, Yazjeen T, Yılmaz MT. EMMSE Strong-Motion Database Serving for Predictive Model Selection to EMMSE Ground-Motion Logic-Tree Applications, Second European Conference on Earthquake Engineering and Seismology, İstanbul, Turkey, Paper No. 3220, 2014.
- [19] Akkar S and Bommer JJ. Influence of long-period filter cut-off on elastic spectral displacements. *Earthq. Eng. Struct. Dynam.* 35, no. 9, 1145-1165, 2006.
- [20] Wells DL and Coppersmith KJ. New empirical relationships among magnitude, rupture length, rupture width, rupture area, and surface displacement. *Bull. Seismol. Soc. Am.* 84, 974-1002, 1994.
- [21] Sandıkkaya MA, Yılmaz MT, Bakır BS, Yılmaz Ö. Site classification of Turkish national strong-motion stations. *Journal of Seismology* 14, 543-563, 2010.
- [22] Türkelli N, E Sandvol, E Zor, R Gok, T Bekler, A Al-Lazki, H Karabulut, S Kuleli, T Eken, C Gurbuz et al.. Seismogenic zones in eastern Turkey. *Geophysical Research Letters* 30, 1–4, 2013.
- [23] Building Seismic Safety Council (BSSC). 2009 NEHRP Recommended Seismic Provisions For New Buildings and Other Structures: Part 1, Provisions, Federal Emergency Management Agency (P-750), Washington, D.C, 2009.

- [24] Abrahamson, N.A., and Youngs, R.R. A stable algorithm for regression analyses using the random effects model, *Bulletin of the Seismological Society of America*, 82, 505-510, 1992.
- [25] Akkar, S. and Cheng, Y. Application of a Monte-Carlo simulation approach for the probabilistic assessment of seismic hazard for geographically distributed portfolio, *Earthquake Engineering and Structural Dynamics*, 45, 525-541, 2016.
- [26] Bohnhoff, M., Bulur, F., Dresen, G., Malin, P., Eken, T. and M. Aktar. An earthquake gap south of Istanbul, *Nature Communications*, 1-6, 2003.
- [27] Steward, J., Chiou, S.J., Bray, J.D., Graves, R.W., Somerville, P.G. and N.A. Abrahamson. Ground motion evaluation procedures for performance-based design. *Pacific Earthquake Engineering Research Center Report PEER 2001/09*, 226p, 2001.
- [28] OYO International Corporation. Updating estimations of the probable earthquake in Istanbul final report. *Production of Microzonation Report and Maps for Asian Side Project*. 251p, 2009.